

# Cellular Automaton Simulation for the Effects of Uneven Distribution of Dislocation Density and Small-Sized Precipitated Particles on Dynamic Recrystallization

X J Guan<sup>1,2,3</sup> and B J Yu<sup>1,2</sup>

<sup>1</sup> Key Laboratory for Liquid-Solid Structural Evolution and Processing of Materials (Ministry of Education), xjguan@sdu.edu.cn, Jinan, 250061, P R China

<sup>2</sup> School of Material Science and Engineering, Shandong University, Jinan, 250061, P R China

**Abstract.** Based on the fundamental metallurgical principles, a modified cellular automaton model which considers the influences of uneven distribution of dislocation density and small-sized precipitated particles was proposed to simulate the dynamic recrystallization (DRX) performances of steels with the three kinds of equivalent particle's size. The results show that the model can truly simulate the nucleation order and multi-round feature of DRX as well as the law of small-sized precipitated particle's retarding DRX; The finer are the particles, the stronger gets the action of their pinning grain boundary.

## 1. Introduction

Dynamic recrystallization (DRX) plays a significant role in thermo-mechanical processing due to its improving mechanical properties by refining grain[1]. In the process of DRX, grain boundary migration decides the mean grain size of microstructure and is retarded by micro-alloying elements in metallic alloys as pinning effect of precipitated particles (Zener pinning)[2].

Many researches have been focused on DRX in recent decades. In these researches, if only the kinetics is of interest, the Johnson-Mehl-Avrami-Kolmogorov (JMAK) approach[3,4] can present a reasonable description. If information on microstructure development during DRX is simultaneously required, the models with adequate temporal and spatial resolution are needed. Therefore, numerical models, such as Q state Monte Carlo (MC)[5,6], phase field (PF)[7] and cellular automaton (CA)[8-15] have been proposed to simulate DRX. Compared with MC and PF method, the CA method is used more because of its more flexible and adaptable to temporal and spatial scale. Goetz and Seetharaman[8] first applied CA method to simulate the DRX features such as the necklace type of microstructures at high strain rates and its kinetics obeying the JMAK equation. Then, many researchers have been focused on DRX simulation based on the CA method[9-15]. However, the investigation with regard to the effects of precipitated particles on DRX is little. This work thoroughly simulates the DRX microstructure evolution in three steels with the different mean sizes and same volume fraction of precipitated particles by using a new CA model, respectively, and discusses the related effects.

## 2. The CA model for DRX

For the sake of simplifying the model, two assumptions are proposed as follows.

(1) The precipitated circular particles randomly distribute in the deformed matrix, and their shape and size do not change with deformation.



(2) For all primary grains and newly formed DRX grains, the dislocation density,  $\rho_0$ , is uniform and identical, and is set as  $10^9/\text{m}^2$ .

Except for the two equations for dislocation density distribution and R-grain growth kinetics, the rest content of the CA-model used in this paper are same as Reference [12].

### 2.1. Dislocation density distribution

If the effects of grain size and its boundary on dislocation density are considered, the mesoscopic dislocation density increment of a cell  $(i, j)$ ,  $\Delta\rho_{i,j}$ , can be expressed as[13]:

$$\Delta\rho_{i,j} = C \cdot \Delta\rho \left( \frac{d_m}{d_{i,j}} \right)^2 \cdot \left[ \frac{1}{k} \sum_{n=1}^k (L_n / d_{CA})^{-2} \right] \quad (1)$$

where  $C$  is a constant to keep the total dislocation density of the simulated region to be invariable;  $\Delta\rho$  is the average dislocation density increment of the simulating region;  $d_m$  is the average grain size of the simulating region;  $d_{i,j}$  is the size of grain cell  $(i, j)$  exists in;  $k$  is the number of grain boundaries of surrounded cell  $(i, j)$ ;  $L_n$  is the distance between cell  $(i, j)$  and its  $n$ th grain boundary;  $d_{CA}$  is lattice constant.

### 2.2. R-grain growth kinetics

After nucleation, the newly formed R-grains will be driven to the deformed matrix of surrounded them by the difference of dislocation density. The velocity of grain boundary moving relates to driving force. Except for the changes of stored energy and grain boundary energy associated with the growth of R-grain, the effects of precipitated particle's pinning grain boundary on the driving force should also be considered in the material with precipitates. So, the driving force,  $\Delta F_{i,j}$ , can be expressed as<sup>[13]</sup>:

$$\Delta F_{i,j} = \tau \Delta\rho_{i,j} - 2 \frac{\gamma_{i,j}}{r_{i,j}} - p_z = \tau \Delta\rho_{i,j} - 2 \frac{\gamma_{i,j}}{r_{i,j}} - \frac{3\gamma_m f_{sec}}{2r_{sec}} \quad (2)$$

where  $\tau$  is the dislocation line energy;  $\rho_{i,j}$ , represents the dislocation density difference between the R-grain and its surrounding matrix;  $\gamma_{i,j}$  and  $r_{i,j}$  are the boundary energy and radius of the R-grain, respectively;  $\gamma_m$  is the energy of the grain boundary with a high-angle (taken as  $15^\circ$ );  $f_{sec}$  and  $r_{sec}$  are the volume fraction and equivalent radius of the precipitated particles, respectively. It is obvious that the third term at right hand of Equation (2) reflects the pinning effect.

### 2.3. Simulation procedure

A 2-D square lattice consisting of  $1500 \times 1500$  cells, corresponding to an area of  $300 \mu\text{m} \times 300 \mu\text{m}$  in the real sample were employed in this study. The presented simulation results were implemented in a CA code written in the Visual Fortran 6 programming language. The initial microstructure with the average grain diameter of some  $48 \mu\text{m}$  was set by a normal grain growth program[14], and the maximum grain orientation number is 180.

A series of simulations for the DRX behaviors of an HPS485wf steel deformed at  $T=1373 \text{ K}$ ,  $\dot{\varepsilon}=0.1 \text{ s}^{-1}$  and  $\varepsilon=0.8$  were carried out. And the steel's experimental data obtained at the same deforming conditions[15] were compared with the simulated one. The states of precipitated particles for the simulations are presented in Table 1, and the corresponding materials are marked as the serial numbers. The other parameters in the simulations are listed in Table 2.

**Table 1.** States of precipitated particles.

Serial number	Volume fraction, $f_{sec}$ (%)	Equivalent radius, $r_{sec}$ (nm)
No. 1	0	0
No. 2	1.5	200
No. 3	1.5	100

**Table 2.** Parameters of material used in the simulations[12].

$T_m$ (K)	$k_B$ (JK <sup>-1</sup> )	$Q_{act}$ (kJmol <sup>-1</sup> )	b (nm)	$M$ (MPa)	$\delta D_b$ (m <sup>3</sup> s <sup>-1</sup> )	$Q_b$ (kJmol <sup>-1</sup> )	$\gamma_m$ (Jm <sup>-2</sup> )
1810	$1.38 \times 10^{-23}$	396.84	0.256	$8.1 \times 10^4$	$7.5 \times 10^{-14}$	159	0.76

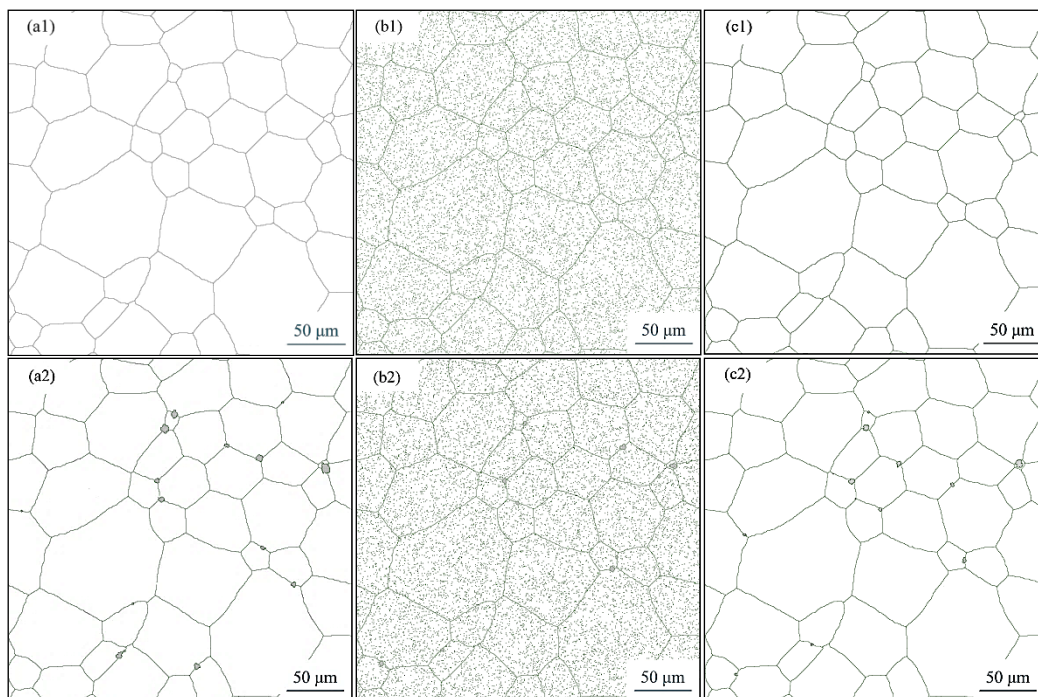
### 3. Results and discussion

It is shown in figure 1 that with increasing strain, R-grains continuously nucleate at the grain boundaries of small-sized grains, then at that of large-sized grains, and gradually grow into surrounding deformed matrix to replace the initial microstructures. Nine circles of DRX occur at the deformation end ( $\epsilon=0.8$ ). It is seen that the improved CA model more truly simulates the DRX performances compared with that of conventional CA simulations.

The simulated and experimental stress-strain curves for No.1, No.2 and No.3 are compared in figure 2(a). The simulated curves show the obvious DRX characteristic with single peak pattern and the values of steady stress corresponding to the some 75% of peak stress ones, which is same as the experimental one. Compared with No.1, the simulated stress-strain curves of No.2 and No.3 are better agreement with the experimental results. It is seen in figure 2(b) that there is a common incubation stage of DRX in the materials before the strain reaches 0.1 and their volume fractions of DRX increase with raising strain, which is also same as the experiment. In addition, the DRX rate of No.1 is faster than that of No.2, and even faster than that of No.3, which is due to the effects of precipitated particles on resisting grain boundary migration. When the volume fraction of precipitated particles is fixed, the smaller is the particle size and the much intensive is their resistance effect. Therefore, the model of considered the small-sized particle's effect is more necessary to the DRX simulation of micro-alloying steel, such as the HPS485wf steel.

In addition, compared with the idea Avrami exponent of JMAK equation,  $n_{Avrami}$ , the values from simulation results also are reasonable, and the effect of precipitated particles on it is little.

In summary, the CA model and its program of this paper not only better simulate the nucleation order and multi-round feature of DRX, but also the more truly reflect the effect of small-sized precipitated particles on DRX performances in the steel.



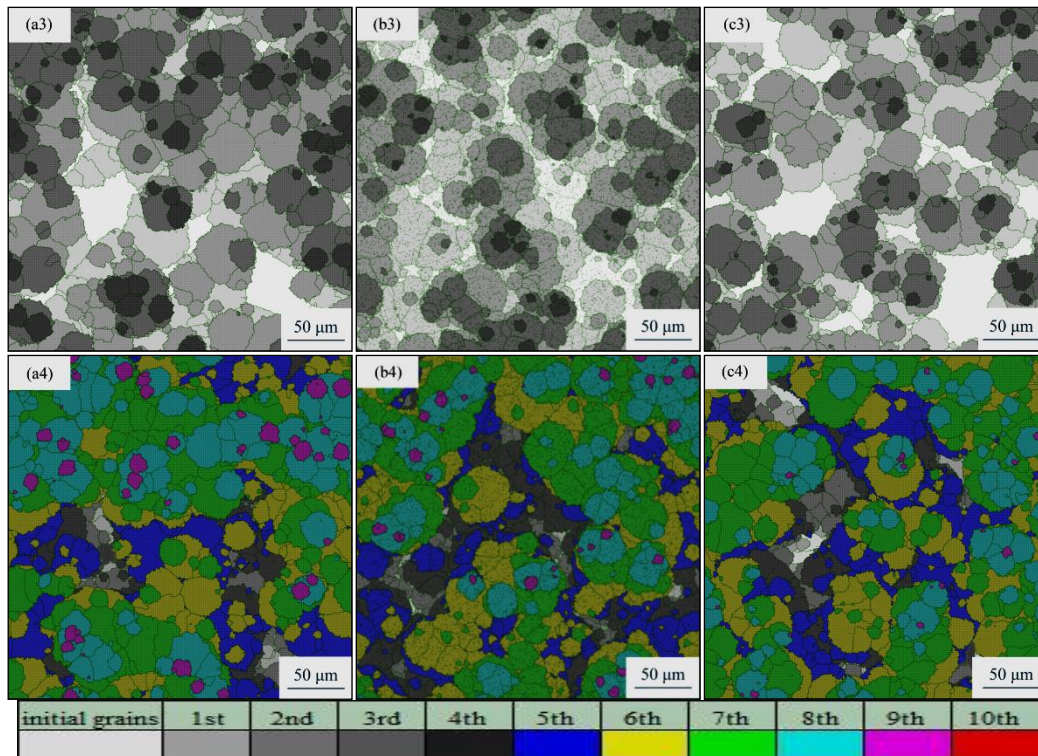


**Figure 1.** Microstructure evolutions of dynamic recrystallization for the materials with different precipitated particles. (a1~a4)  $r_{\text{sec}}=0$  nm,  $f_{\text{sec}}=0$ ; (b1~b4)  $r_{\text{sec}}=200$  nm,  $f_{\text{sec}}=0.015$ ; (c1~c4)  $r_{\text{sec}}=100$  nm,  $f_{\text{sec}}=0.015$ ; (a1, b1, c1)  $\varepsilon=0$ ; (a2, b2, c2)  $\varepsilon=0.1$ ; (a3, b3, c3)  $\varepsilon=0.4$ ; (a4, b4, c4)  $\varepsilon=0.8$ .

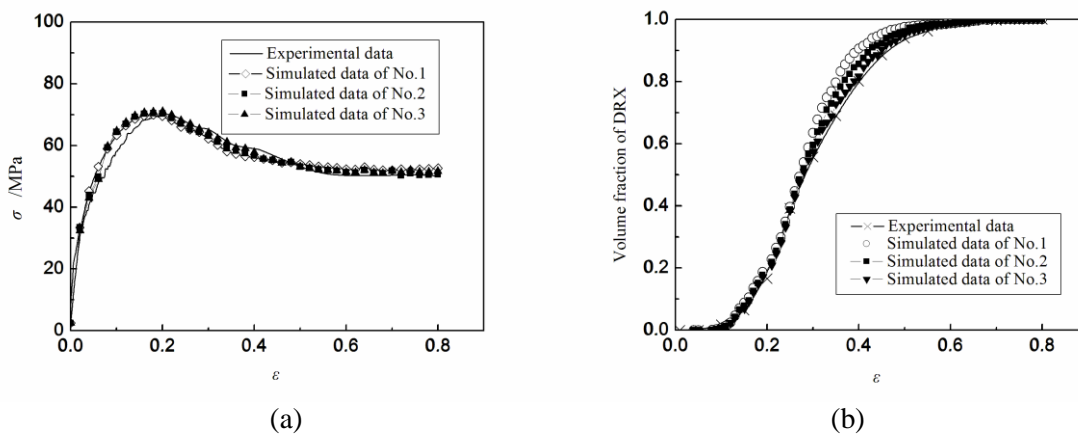


**Figure 2.** Stress-strain curves and kinetics of dynamic recrystallization for the materials with different precipitated particles (a) Stress-strain curves (b) kinetics.

#### 4. Conclusions

A modified CA model is successfully used for simulating the two effects of finer precipitated particles on DRX, that is, the dislocation accumulating and the grain boundary migration resisting, which expresses the more real nucleation order and multi-round feature of DRX as well as the correct law of small-sized particle's pinning R-grain boundary. The resisting action strengthens with the decrease of the small-sized particle's average size at the same volume fraction, but do not affect the nucleation behaviors of DRX.

## 5. References

- [1] Montheillet F, Lurdos O and Damamme G 2009 A grain scale approach for modeling steady-state discontinuous dynamic recrystallization *Acta. Mater.* **57** 1602-12
- [2] Semiatin S L, Weaver D S, Fagin P N, Glavicic M G, Goetz R L, Frey N D, Krumb R C and Anthony M M 2004 Deformation and recrystallization behavior during hot working of a coarse-grain nickel-based superalloy ingot material *Metall. Mater. Trans. A* **35** 679-93
- [3] Avrami M 1939 Kinetics of phase change I: general theory, *J. Chem. Phys.* **7** 1103-12
- [4] Jonas J J, Queleennec X and Jiang L 2009 The Avrami kinetics of dynamic recrystallization, *Acta. Mater.* **57** 2748-56
- [5] Rollett A D, Luton M J and Srolovitz D J 1992 Microstructural simulation of dynamic recrystallization *Acta. Metall. Mater.* **40** 43-55
- [6] Peczak P 1995 A Monte Carlo study of influence of deformation temperature on dynamic recrystallization *Acta. Metall. Mater.* **43** 1279-91
- [7] Takaki T, Hisakuni Y and Hirouchi T 2009 Multi-phase-field simulations for dynamic recrystallization *Comput. Mater. Sci.* **45** 881-88
- [8] Goetz R L and Seetharaman V 1998 Modeling dynamic recrystallization using cellular automata *Scrip. Mater.* **38** 405-13
- [9] Ding R and Guo Z X 2001 Coupled quantitative simulation of microstructural evolution and plastic flow during dynamic recrystallization *Acta. Mater.* **49** 3163-75
- [10] Lee H W and Im Y T 2010 Cellular automata modeling of grain coarsening and refinement during the dynamic recrystallization of pure copper *Mater. Trans.* **51** 1614-20
- [11] Guan X J and Yu B J 2013 Simulation of the dynamic recrystallization in HPS485wf steel deformed at different conditions *J. Xuzhou Inst. Techno.* **28** 1-4
- [12] Guan X J, Yu B J, Wang L J, Zhou L J and FU J 2014 Simulation of dynamic recrystallization for advanced steel HPS485wf using cellular automata *Trans. Mater. Heat Treat.* **35** 218-24
- [13] Yu B J 2012 Modeling and simulation of dynamic recrystallization behavior for material with second phase particles using cellular automata method *Doctoral Dissertation* (Jinan: Shandong University) pp 69-72
- [14] Ma X F, Guan X J, Liu Y T, Shen X M, Wang L J, Song S T and Zeng Q K 2008 Cellular automaton model for grain growth based on modified transition rule *Chin. J. Nonferrous Met.* **189** 138-44
- [15] Wang L J, Guan X J, Zhao J, Yu B J, Zeng Q K, Sun Q and Liu Q Q 2010 Dynamic recrystallization and mathematic model of HPS482wf steel *Trans. Mater. Heat Treat.* **31** 147-51

## Acknowledgements

We sincerely acknowledged the support from the Specialized Research Fund for Doctoral Program of Higher Education of China (No.200804220021).